J. Water Environ. Nanotechnol., 4(2): 147-156 Spring 2019

ORIGINAL RESEARCH PAPER

The adsorption of sulfur dioxide and ozone molecules on boron nitride nanotubes: A DFT study

***Amirali Abbasi*[1,2,3]**

[1] *Molecular Simulation laboratory (MSL), Azarbaijan Shahid Madani University, Tabriz, Iran*
[2] *Computational Nanomaterials research group (CNRG), Azarbaijan Shahid Madani University, Tabriz, Iran*
[3] *Department of Chemistry, Faculty of Basic Sciences, Azarbaijan Shahid Madani University, Tabriz, Iran*

Received: 2019-02-14 Accepted: 2019-04-12 Published: 2019-05-01

ABSTRACT

Density functional theory calculations were carried out to investigate the adsorption behaviors and electronic structures of SO_2 and O_3 molecules on the pristine boron nitride nanotubes. The structural and electronic properties of the studied systems were investigated in view of the adsorption energies, band structures, and molecular orbitals. Various adsorption positions of gas molecules on the boron nitride nanotubes were examined in detail. The band structure calculations indicate that the pristine BN nanotube works as a wide band gap semiconductor, and can be applied as an efficient candidate for SO_2 and O_3 sensing purposes. NBO analysis reveals that SO_2 acts as a charge donor, whereas O_3 molecule behaves as a charge acceptor from the BN nanotube. Molecular orbital calculations indicate that the LUMOs were dominant on the nanotube surface, whereas the electronic densities in the HOMOs were mainly distributed over the adsorbed SO_2 and O_3 molecules. Moreover, the charge density difference calculations indicate charge accumulation on the adsorbed gas molecule.

Keywords: *Adsorption; BN Nanotube; Charge Density Difference, DFT; Gas Molecule*

How to cite this article
Abbasi A. The adsorption of sulfur dioxide and ozone molecules on boron nitride nanotubes: A DFT study. J. Water Environ. Nanotechnol., 2019; 4(2): 147-156. DOI: 10.22090/jwent.2019.02.006

INTRODUCTION

The suggestion of efficient strategies for monitoring and reduction of environmental pollutants are very essential in biological and industrial processes. In the past few years, a huge surge of attention has been devoted to the design and improvement of appropriate gas sensing materials and harmful chemical remover devices [1-3]. Sulfur dioxide (SO_2) is one of the main contributors to air pollution, which comes from exhaust products. Ozone (O_3) has been also considered as harmful gas to the respiratory tissues and ocular mucosa, being mostly introduced to the human body by inhalation. The main target of tropospheric ozone is the lung. Also, it causes detrimental impacts on the eyes and the nervous system [4]. Consequently, ozone has long been considered one of the most dangerous air pollutants. Under solar light, the NO_x gases emitted from vehicle engines, power plants and volatile organic compounds in factory waste gas contribute to a photochemical reaction to create photochemical smog and ozone molecule. Therefore, the quick and precise detection of ozone to control its emission at the atmosphere is a key subject that should be resolved and fixed [5]. Thus, it is of eminent importance to decrease or remove toxic SO_2 and O_3 molecules from the atmosphere. The most effective way to decrease or eliminate these air pollutants is the use of some gas sensors or removers. In this regard, BN nanotubes have been considered to be efficient sensing materials, which can be utilized for monitoring the concentrations of these gases in the air.

Carbon nanotubes (CNTs) were first discovered by Iljima [6] and were demonstrated to be used in a wide range of applications [7-11]. Boron

* Corresponding Author Email: *a_abbasi@azaruniv.ac.ir*

nitride nanotubes which possess a similar geometry with carbon nanotubes have attracted significant attention in the past decades [12-21]. Owing to the unique mechanical properties, satisfied thermal conductivity, and high chemical stability [22], BN nanotubes have been proven to be promising material candidates for applications in nano-electronic devices and nanomedicine [23, 24]. Their properties can be modified by introducing different functional groups to wrap around with covalent or non-covalent interactions, which leads to the exceptional properties of BN nanotubes [25].

In comparison with carbon nanotubes, BN nanotubes have more advantages as they possess small toxicity. Besides, their electronic properties are independent of the diameter and chirality. The characteristics such as great surface to volume ratios and the high chemical stability make semiconducting BN nanotubes sensitive materials. Gas sensing materials, which were constructed from BN nanotubes have aroused significant attention because of their outstanding sensing capabilities [26-30]. Since the discovery of BN nanotubes, a large number of theoretical and experimental studies are carried out to examine the gas sensing capability of BN nanotube-based sensors [30, 31]. Furthermore, element doped BN nanotubes show advantages such as improved conductivity and chemical reactivity and sensor properties compared to the pristine ones [32-34]. Performing DFT calculations, Wang et al. suggested that the adsorption performance of BN nanotubes towards CH_2O can be amended by Si doping [35]. Several works have been carried out, describing the adsorption behaviors of TiO_2 semiconductor based nanoparticles and nanocomposites [36-45] and two-dimensional stanene nanosheets [46]. Besides, the adsorption energy of both SO_2 and O_3 on BNNT were compared with those of other adsorbents [47-54]. The exceptional sensor properties of BN nanotubes encourages us to examine the sensor properties of these nanotubes towards SO_2 and O_3 detection. In this paper, we performed a systematical first-principles study to investigate the interactions of SO_2 and O_3 gases with the pristine single-walled BN nanotubes. The main aim of this study is to explore the favorable materials for detecting harmful SO_2 and O_3 molecules in the atmosphere. The structural and electronic properties of the adsorption systems were mainly analyzed in view of the adsorption energies, charge density difference, molecular orbitals and Kohn-Sham, Hartree-Fock potentials.

METHODOLOGY AND MODEL SYSTEMS

All calculations were performed using the density functional theory (DFT) [55, 56], as implemented in the open source package for material eXplorer (OPENMX3.8) package [57]. The generalized gradient approximation (GGA) in the Perdew-Burke-Ernzerhof (PBE) format was used to describe the exchange-correlation potentials [58]. The pseudo-atomic orbitals (PAOs) centered on atomic sites were used as basis sets. The chosen basis sets were specified by S8.0-s3p3, O5.0-s2p2, B7.0-s2p2, and N5.0-s2p2, in generation by a confinement scheme. In our calculations, the energy cutoff was set to 150 Ry. For the considered BN nanotube, we have considered a (6, 6) nanotube. The convergence criterion for the self-consistent electronic minimization was set to 10^{-6} Hartree, and the force acting on each atom converges to 0.01 eV $Å^{-1}$. The open-source program XCrysDen [59] was used for the visualization of adsorption configurations of BN nanotubes with adsorbed SO_2 and O_3 molecules. Also, VESTA (visualization for electronic and structural analysis) program was employed for visualization of the volumetric data such as electron/nuclear densities [60]. Besides, the adsorption energy is estimated based on a difference between the total energy of the complex BN+Adsorbate system and individual BN and gas molecule components.

Thus, the adsorption energy (ΔE_{ad}) is estimated using the following formula:

$$\Delta E_{ad} = E_{molecule/nanotube} - E_{molecule} - E_{nanotube} \quad (1)$$

where, $E_{molecule/nanotube}$, $E_{molecule}$, and $E_{nanotube}$ are the total energies of BN nanotube with the adsorbed gas molecule, free gas molecule and bare BN nanotube, respectively.

RESULTS AND DISCUSSION

To identify the most stable adsorption configurations of SO_2 and O_3 molecules on the surface of BN nanotubes, we have examined three orientations of each of the SO_2 and O_3 molecules towards the nanotube surface. The relaxed structures of the considered BN nanotubes with adsorbed gas molecules were shown in Fig. 1.

The different atoms of the BN nanotubes were considered to be the active adsorption sites on the surface. Therefore, three types of initial adsorption structures of SO_2 on the nanotube were considered: (A) SO_2 molecule is perpendicular to the BN

nanotube with two oxygen atoms positioned downward, which are located towards the boron atoms of the BN nanotube.

In this configuration, oxygen atoms of SO_2 molecule were initially placed at the top of the boron atoms with a maximum distance of 2.02 Å with respect to the nanotube surface; (B) SO_2 molecule is perpendicular to the nanotube with two oxygen atoms positioned at the top of the boron and nitrogen atoms of the nanotube, and this configuration presents a downward orientation of SO_2 over the surface, the average distance between the nanotube and SO_2 molecule is about 2.05 Å.; (C) SO_2 molecule is perpendicular to the surface with oxygen atoms oriented at the top of the nitrogen atoms of the nanotube, the oxygen atom was weakly adsorbed on the surface of BN nanotube. In this configuration, we can see that SO_2 stands in a distance of 2.08 Å above the nanotube surface. For O_3 adsorption on the surface of BN nanotube, we can also consider three configurations denoted by adsorption types D-F. Among three configurations for SO_2 adsorption on the BN nanotubes, configuration A has the lowest value of adsorption distance, representing the relative orientation of SO_2 over the boron atoms of the nanotube, whereas the highest value of distance belongs to configuration C. The variation trends of adsorption energies show inverse relation with adsorption distances. The average value of adsorption energy for SO_2 adsorption on the BN nanotube is about 0.32 eV.

(D) O_3 molecule is perpendicular to the surface of BN nanotube with side oxygen atoms located downward, which are placed towards the boron atoms of the BN nanotube. The central oxygen atom of the nanotube does not contribute to the adsorption anymore. Instead, the side oxygen atoms were tested to be the most favorable adsorption sites. The average distance of O_3 molecule towards the BN nanotube is about 2.03 Å, which makes it the most favorable and strongest adsorption configuration.; (E) O_3 molecule is suited perpendicularly to the nanotube surface with side oxygen atoms located at the top of the boron and nitrogen atoms of the nanotube, Similarly, in this configuration, the central oxygen atom of the O_3 molecule does not interact with the nanotube; and the distance is about 2.06 Å.; (F) O_3 molecule is perpendicular to the surface with side oxygen atoms adapted to the nitrogen atoms of the nanotube. In this configuration, the side oxygen

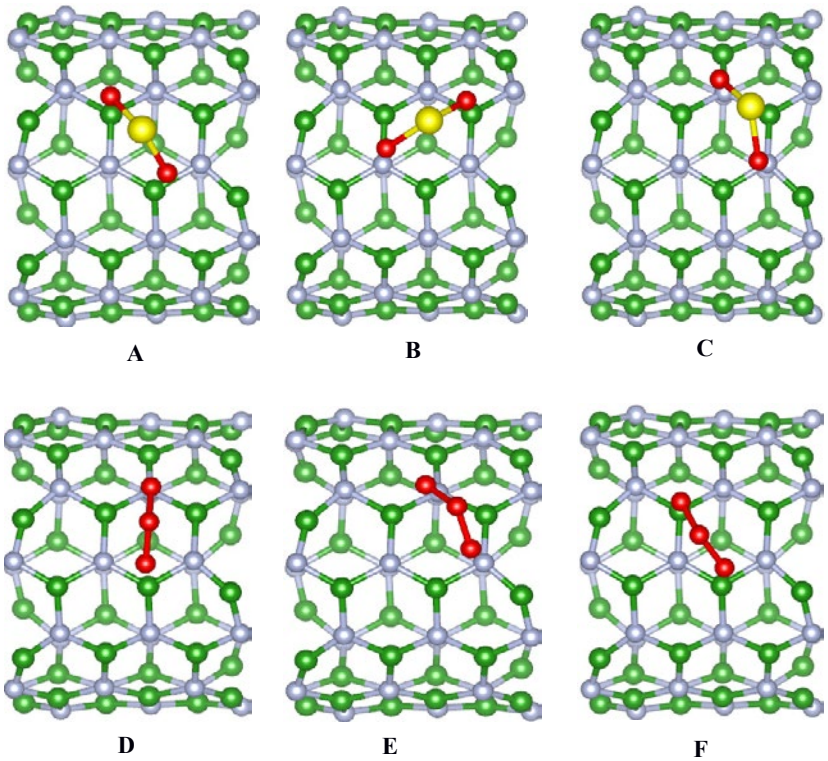

Fig. 1. Optimized geometry configurations of SO_2 and O_3 molecules adsorbed on the boron nitride (BN) nanotubes.

atoms weakly interact with the nitrogen atoms of the nanotube, and the resultant distance between the nanotube and O_3 molecule is about 2.11 Å. Of the three configurations for O_3 adsorption on the BN nanotube, configuration D presents the smallest distance between the nanotube and O_3 molecule, while the largest distance belongs to configuration F. The average adsorption energy is about 0.25 eV. Configuration D represents the strongest interaction between the nanotube and O_3 molecule since it shows the least distance of O_3 towards the nanotube surface.

All of these configurations represent the physical adsorption (physisorption) of the gas phase SO_2 and O_3 molecules on the nanotube surface as the substrate weakly interact with the adsorbing gas molecules. For all configurations, we found that the S-O and O-O bonds of the SO_2 and O_3 molecules were slightly elongated after the adsorption process. The reason can be probably attributed to the transfer of electronic density from the nanotube surface to the gas molecules, making their bond lengths stretched.

Fig. 2 displays the electronic band structures of the considered unit cell and supercell of (6, 6) BN nanotube, which represents that BN nanotube acts as a large bandgap semiconductor. It is well known to the sensor community that the semiconductor characteristics of the sensor material are an essential feature. Thus, the considered (6, 6) BN nanotube behaves as an appropriate sensor material due to its wide band gap and semiconducting nature. Figs.s 3 and 4 show the band structures for SO_2 and O_3 adsorbed BN nanotubes. It can be seen from these Figures that the electronic structure of the nanotubes was not significantly changed upon adsorption of gas molecules. The only change is the creation of a small line above the valence band edge of nanotubes. Therefore, the electronic band structures of the BN nanotubes remain unaffected after the adsorption of gas molecules. This is in accordance with the weak physisorption of the gas molecule on the nanotube surface.

The isosurface plots of the highest occupied molecular orbitals (HOMOs) and the lowest unoccupied molecular orbitals (LUMOs) for SO_2 adsorption on the considered BN nanotubes were displayed in Fig. 5. As can be seen from this figure, the LUMOs of the adsorption systems are dominant over the adsorbed gas molecules, whereas the electronic density in the HOMOs is mainly distributed on the nanotube surface. The molecular orbitals of the SO_2 molecule on the BN nanotube are in reasonable agreement with the calculated Kohn-Sham and Hartree-Fock potentials for the considered systems (Fig. 6). Similarly, Fig. 7 presents the isosurface plots of HOMOs and LUMOs for O_3 adsorption on the considered BN nanotubes. These figures also show that the LUMOs are mostly located over the adsorbed O_3 molecule, while the electronic densities in the HOMOs are high at the nanotube

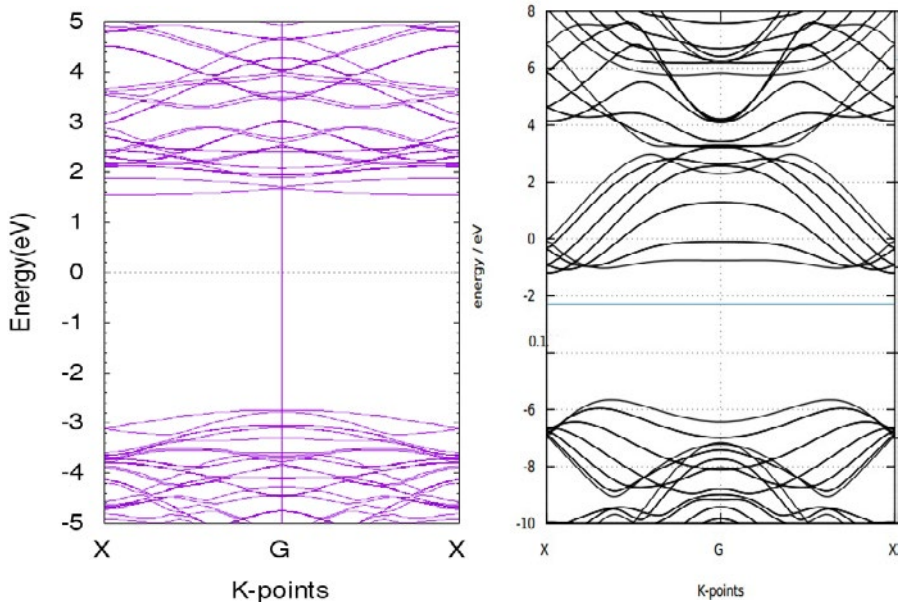

Fig. 2. Electronic band structures for the unit cell and supercell of the considered BN nanotube.

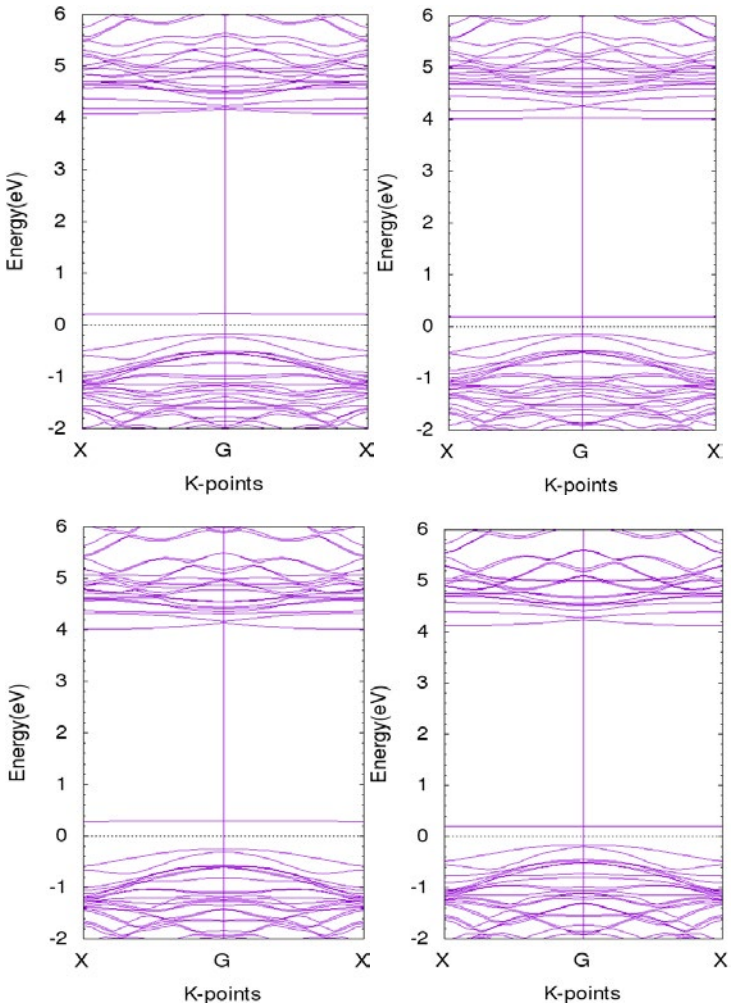

Fig. 3. Electronic band structures for the SO_2 adsorbed and O_3 adsorbed BN nanotubes.

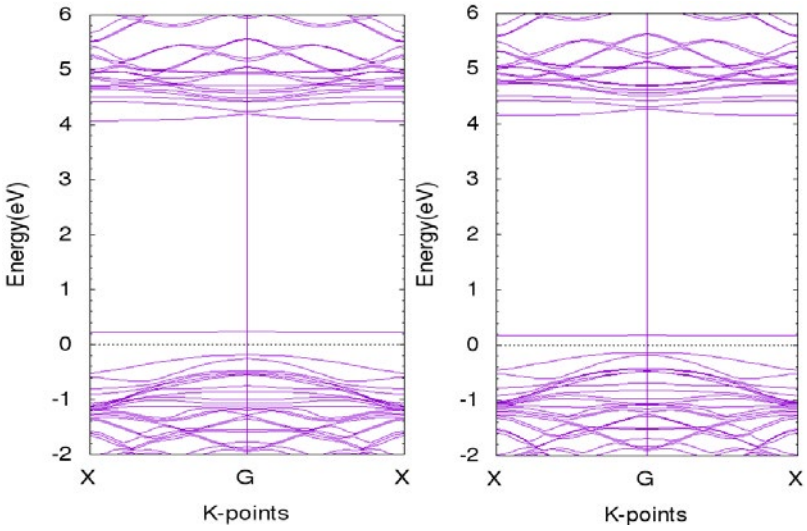

Fig. 4. Electronic band structures for the SO_2 adsorbed and O_3 adsorbed BN nanotubes.

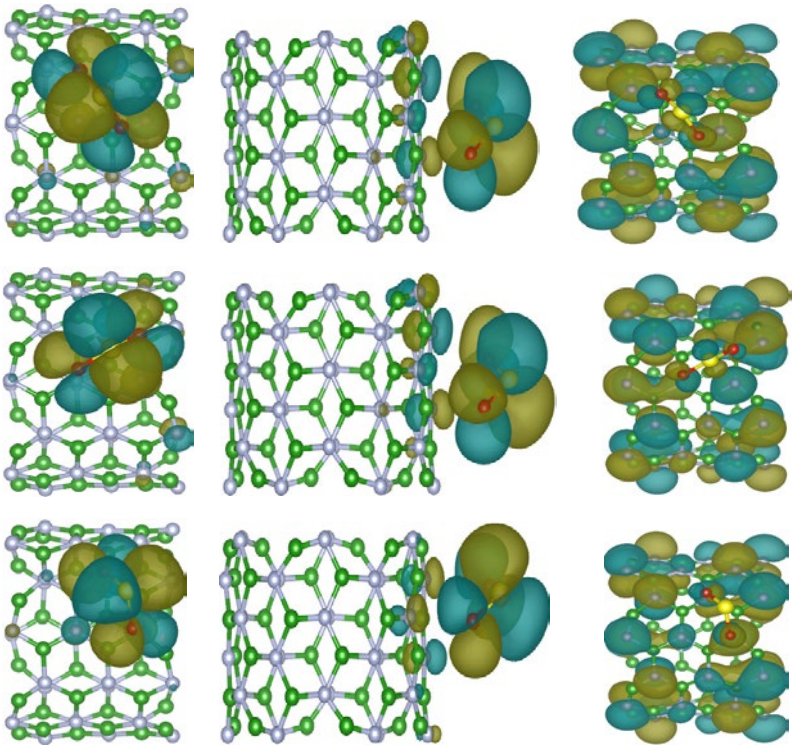

Fig. 5. Isosurface plots of HOMOs and LUMOs for SO_2 adsorbed BN nanotubes.

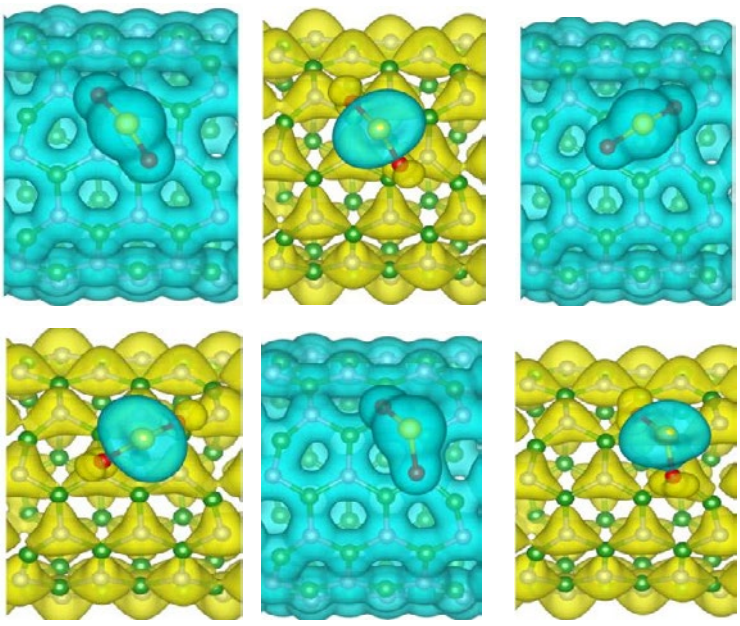

Fig. 6. Calculated Kohn-Sham and Hartree-Fock potential Isosurfaces for SO_2 adsorbed BN nanotubes.

surface. The calculated potentials for O_3 molecule adsorption on the nanotube were also displayed in Fig. 8, which indicates the potential distribution of the whole system consisting of the BN nanotube and its adsorbed gas phase O_3 molecule.

In order to further examine the electronic structure of the interaction of gas molecules with BN nanotubes, we have presented the isosurfaces of the charge density difference plots for O_3 adsorption on the considered nanotubes. As can be seen from

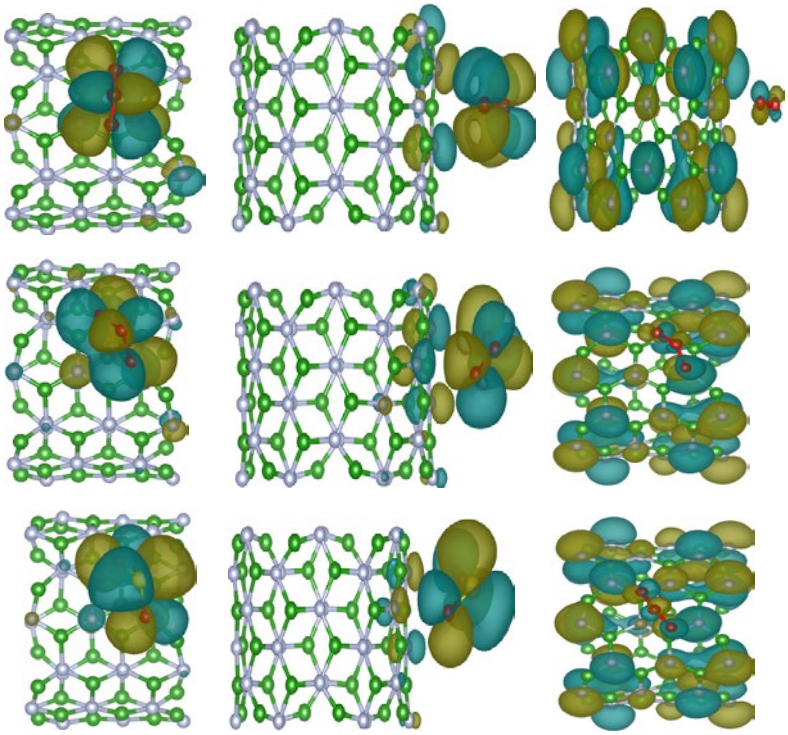

Fig. 7. Isosurface plots of HOMOs and LUMOs for O_3 adsorbed BN nanotubes.

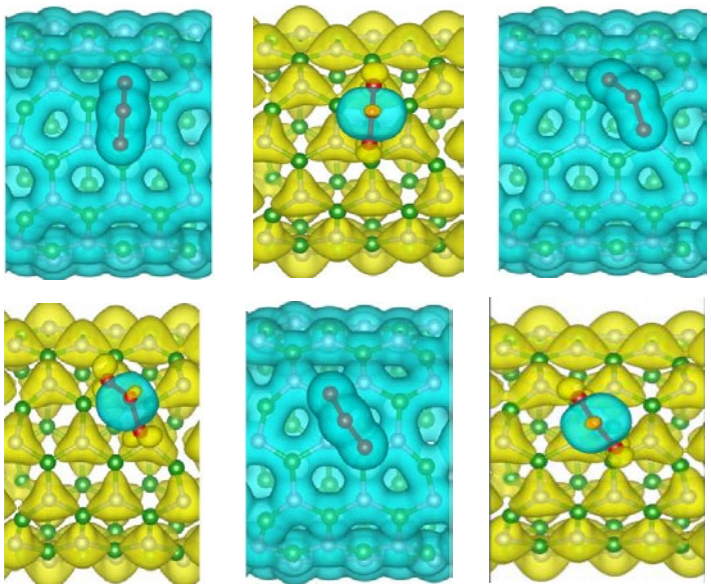

Fig. 8. Calculated Kohn-Sham and Hartree-Fock potential Isosurfaces for O_3 adsorbed BN nanotubes.

these figures, there is a charge accumulation on the adsorbed O_3 molecule after the adsorption process. Thus, O_3 adsorption affects the electronic properties of the complex system by concentrating the electronic charges on the adsorbed gas molecule.

The natural bond orbital (NBO) analysis was conducted in this work in order to gain further insights into the charge transfer between adsorbent and adsorbate. The adsorption of O_3 and SO_2 makes substantial changes in the electronic behaviors of BN nanotube-based sensors. The SO_2 molecule gives charges to the BN nanotube, whereas O_3

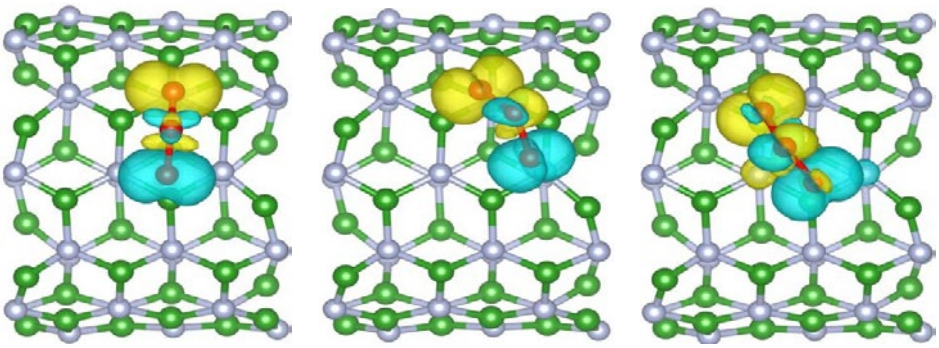

Fig. 9. Isosurface plots of charge density differences for O_3 molecule adsorbed on the considered nanotubes.

molecule acts as a charge acceptor and accepts a charge from the BN nanotube. NBO analysis reveals a noticeable average charge transfer of about -0.32 |e| (e, the electron charge) from BN nanotube to O_3 molecule. For SO_2 adsorption on the nanotube, the average charge transfer from SO_2 to the BN nanotube is calculated to be -0.28 |e|

CONCLUSIONS

In this paper, we have performed density functional theory calculations to investigate the adsorption behaviors of gas phase SO_2 and O_3 molecules on the considered BN nanotubes. We have examined different adsorption positions of the gas molecules on the nanotube surface. The results suggest that the adsorption of SO_2 and O_3 molecules on the pristine BN nanotube is an energy-favorable process. After the adsorption process, the S-O and O-O bonds of the adsorbed SO_2 and O_3 molecules were lengthened. The reason is that the electronic density transfers from the old bonds of the adsorbed SO_2 and O_3 molecules to the nanotube surface, making their bond lengths elongated. Molecular orbital calculations indicate that the electronic densities in the LUMOs were mainly distributed over the adsorbed gas molecules, whereas the HOMOs were high at the BN nanotube, as evidenced by the isosurface plots of Kohn-Sham potentials. NBO analysis reveals that SO_2 acts as a charge donor, whereas O_3 molecule behaves as a charge acceptor from the BN nanotube. The charge density difference calculations indicate the accumulation of electronic density over the adsorbed O_3 molecules, which suggest that O_3 acts as an acceptor agent from the BN nanotube. This work aims at providing a theoretical basis and understanding of the adsorption behaviors of BN based chemical sensors for the detection of harmful gas molecules in the environment

ACKNOWLEDGMENT

This work has been supported by Azarbaijan Shahid Madani University.

CONFLICT OF INTEREST

The authors declare that there are no conflicts of interest regarding the publication of this manuscript.

REFERENCES

1. Air pollution control technology, Bretschneider, B., and Kurfurso, J. Elsevier, Amsterdam, 1987, $75.50, 297 pgs. Environmental Progress. 1987;6(3):A7-A.
2. N. Fiedler, R. Laumbach, K. Kelly-McNeil, P. Lioy, Z.-H Fan, J. Zhang, J. Ottenweller, P. Ohman-Strickland, H. Kipen, Environ. Health Perspect. 2005, 113, 1542.
3. K. J. Lee, N. Shiratori, G.H. Lee, J. Miyawaki, I. Mochida, S.-H. Yoon, J. Jang, Carbon 48 (2010) 4248.
4. Felix EP, Filho JP, Garcia G, Cardoso AA. A new fluorescence method for determination of ozone in ambient air. Microchemical Journal. 2011;99(2):530-4.
5. Pisarenko AN, Spendel WU, Taylor RT, Brown JD, Cox JA, Pacey GE. Detection of ozone gas using gold nanoislands and surface plasmon resonance. Talanta. 2009;80(2):777-80.
6. Iijima S. Helical microtubules of graphitic carbon. Nature. 1991;354(6348):56-8.
7. Zhu Z. An Overview of Carbon Nanotubes and Graphene for Biosensing Applications. Nano-Micro Letters. 2017;9(3).
8. Xia Y, Liu M, Wang L, Yan A, He W, Chen M, et al. A visible and colorimetric aptasensor based on DNA-capped single-walled carbon nanotubes for detection of exosomes. Biosensors and Bioelectronics. 2017;92:8-15.
9. Hassan RYA, El-Attar RO, Hassan HNA, Ahmed MA, Khaled E. Carbon nanotube-based electrochemical biosensors for determination of Candida albicans's quorum sensing molecule. Sensors and Actuators B: Chemical. 2017;244:565-70.
10. Lan L, Yao Y, Ping J, Ying Y. Recent advances in nanomaterial-based biosensors for antibiotics detection. Biosensors and Bioelectronics. 2017;91:504-14.
11. D'Acunto M, Colantonio S, Moroni D, Salvetti O. Detection limit of biomarkers using the near-infrared band-gap fluorescence of single-walled carbon nanotubes. Journal of Modern Optics. 2010;57(18):1695-9.

12. Sundaram R, Scheiner S, Roy AK, Kar T. Site and chirality selective chemical modifications of boron nitride nanotubes (BNNTs) via Lewis acid–base interactions. Physical Chemistry Chemical Physics. 2015;17(5):3850-66.
13. Esrafili MD, Nurazar R. A DFT study on the possibility of using boron nitride nanotubes as a dehydrogenation catalyst for methanol. Applied Surface Science. 2014;314:90-6.
14. Azizi K, Salabat K, Seif A. Methane storage on aluminum-doped single wall BNNTs. Applied Surface Science. 2014;309:54-61.
15. Shao P, Kuang X-Y, Ding L-P, Yang J, Zhong M-M. Can CO2 molecule adsorb effectively on Al-doped boron nitride single walled nanotube? Applied Surface Science. 2013;285:350-6.
16. Farmanzadeh D, Ghazanfary S. Interaction of vitamins B3 and C and their radicals with (5, 0) single-walled boron nitride nanotube for use as biosensor or in drug delivery. Journal of Chemical Sciences. 2013;125(6):1595-606.
17. Baei MT, Peyghan AA, Bagheri Z. A density functional theory study on acetylene-functionalized BN nanotubes. Structural Chemistry. 2012;24(4):1007-13.
18. Beheshtian J, Peyghan AA, Bagheri Z. Detection of phosgene by Sc-doped BN nanotubes: A DFT study. Sensors and Actuators B: Chemical. 2012;171-172:846-52.
19. Zhang LP, Wu P, Sullivan MB. Hydrogen Adsorption on Rh, Ni, and Pd Functionalized Single-Walled Boron Nitride Nanotubes. The Journal of Physical Chemistry C. 2011;115(10):4289-96.
20. Ju S-P, Wang Y-C, Lien T-W. Tuning the electronic properties of boron nitride nanotube by mechanical uni-axial deformation: a DFT study. Nanoscale Research Letters. 2011;6(1).
21. Baei MT, Kaveh F, Torabi P, Sayyad- Alangi SZ. Adsorption Properties of Oxygen onH-Capped (5, 5) Boron Nitride Nanotube (BNNT)- A Density Functional Theory. E-Journal of Chemistry. 2011;8(2):609-14.
22. Blase X, Rubio A, Louie SG, Cohen ML. Stability and Band Gap Constancy of Boron Nitride Nanotubes. Europhysics Letters (EPL). 1994;28(5):335-40.
23. Chen X, Wu P, Rousseas M, Okawa D, Gartner Z, Zettl A, et al. Boron Nitride Nanotubes Are Noncytotoxic and Can Be Functionalized for Interaction with Proteins and Cells. Journal of the American Chemical Society. 2009;131(3):890-1.
24. Ciofani G, Raffa V, Menciassi A, Dario P. Preparation of Boron Nitride Nanotubes Aqueous Dispersions for Biological Applications. Journal of Nanoscience and Nanotechnology. 2008;8(12):6223-31.
25. Lu YH, Chen W, Feng YP, He PM. Tuning the Electronic Structure of Graphene by an Organic Molecule. The Journal of Physical Chemistry B. 2009;113(1):2-5.
26. Yoosefian M, Etminan N, Moghani MZ, Mirzaei S, Abbasi S. The role of boron nitride nanotube as a new chemical sensor and potential reservoir for hydrogen halides environmental pollutants. Superlattices and Microstructures. 2016;98:325-31.
27. Soltani A, Raz SG, Rezaei VJ, Dehno Khalaji A, Savar M. Ab initio investigation of Al- and Ga-doped single-walled boron nitride nanotubes as ammonia sensor. Applied Surface Science. 2012;263:619-25.
28. Wang R, Zhang D, Liu Y, Liu C. A theoretical study of silicon-doped boron nitride nanotubes serving as a potential chemical sensor for hydrogen cyanide. Nanotechnology. 2009;20(50):505704.
29. Solimannejad M, Noormohammadbeigi M. Boron nitride nanotube (BNNT) as a sensor of hydroperoxyl radical (HO2): A DFT study. Journal of the Iranian Chemical Society. 2016;14(2):471-6.
30. Arshadi S, Pourkhiz F. NBO, AIM, and TD-DFT assisted screening of BNNT optimum diameter on ethyl phosphorodimethylamidocyanidate sensor design. Phosphorus, Sulfur, and Silicon and the Related Elements. 2016;191(7):1013-21.
31. Ganji MD, Rezvani M. Boron nitride nanotube based nanosensor for acetone adsorption: a DFT simulation. Journal of Molecular Modeling. 2012;19(3):1259-65.
32. Tontapha S, Ruangpornvisuti V, Wanno B. Density functional investigation of CO adsorption on Ni-doped single-walled armchair (5,5) boron nitride nanotubes. Journal of Molecular Modeling. 2012;19(1):239-45.
33. Zhao J-x, Ding Y-h. Theoretical Study of Ni Adsorption on Single-Walled Boron Nitride Nanotubes with Intrinsic Defects. The Journal of Physical Chemistry C. 2008;112(15):5778-83.
34. Baierle RJ, Piquini P, Schmidt TM, Fazzio A. Hydrogen Adsorption on Carbon-Doped Boron Nitride Nanotube. The Journal of Physical Chemistry B. 2006;110(42):21184-8.
35. Wang R, Zhu R, Zhang D. Adsorption of formaldehyde molecule on the pristine and silicon-doped boron nitride nanotubes. Chemical Physics Letters. 2008;467(1-3):131-5.
36. Abbasi A, Jahanbin Sardroodi J. Modified N-doped TiO 2 anatase nanoparticle as an ideal O 3 gas sensor: Insights from density functional theory calculations. Computational and Theoretical Chemistry. 2016;1095:15-28.
37. Abbasi A, Jahanbin Sardroodi J. N-doped TiO2 anatase nanoparticles as a highly sensitive gas sensor for NO2 detection: insights from DFT computations. Environmental Science: Nano. 2016;3(5):1153-64.
38. Abbasi A, Sardroodi JJ. A novel strategy for SO x removal by N-doped TiO 2 /WSe 2 nanocomposite as a highly efficient molecule sensor investigated by van der Waals corrected DFT. Computational and Theoretical Chemistry. 2017;1114:8-19.
39. Abbasi A, Jahanbin Sardroodi J. Prediction of a highly sensitive molecule sensor for SOx detection based on TiO2/MoS2 nanocomposites: a DFT study. Journal of Sulfur Chemistry. 2016;38(1):52-68.
40. Abbasi A, Jahanbin Sardroodi J. An innovative gas sensor system designed from a sensitive nanostructured ZnO for the selective detection of SOx molecules: a density functional theory study. New J Chem. 2017;41(21):12569-80.
41. Abbasi A, Sardroodi JJ. Theoretical study of the adsorption of NOx on TiO2/MoS2 nanocomposites: a comparison between undoped and N-doped nanocomposites. Journal of Nanostructure in Chemistry. 2016;6(4):309-27.
42. Abbasi A, Sardroodi JJ. Investigation of the adsorption of ozone molecules on TiO2/WSe2 nanocomposites by DFT computations: Applications to gas sensor devices. Applied Surface Science. 2018;436:27-41.
43. Abbasi A, Sardroodi JJ. Adsorption of toxic SOx molecules on heterostructured TiO2/ZnO nanocomposites for gas sensing applications: a DFT study. Adsorption. 2017;24(1):29-41.
44. Abbasi A, Sardroodi JJ, Ebrahimzadeh AR, Yaghoobi M. Theoretical study of the structural and electronic

properties of novel stanene-based buckled nanotubes and their adsorption behaviors. Applied Surface Science. 2018;435:733-42.
45. Abbasi A, Sardroodi JJ. Molecular design of O3 and NO2 sensor devices based on a novel heterostructured N-doped TiO2/ZnO nanocomposite: a van der Waals corrected DFT study. Journal of Nanostructure in Chemistry. 2017;7(4):345-58.
46. Abbasi A, Sardroodi JJ. Density functional theory investigation of the interactions between the buckled stanene nanosheet and XO2 gases (X = N, S, C). Computational and Theoretical Chemistry. 2018;1125:15-28.
47. Rad AS, Nasimi N, Jafari M, Shabestari DS, Gerami E. Ab-initio study of interaction of some atmospheric gases (SO2, NH3, H2O, CO, CH4 and CO2) with polypyrrole (3PPy) gas sensor: DFT calculations. Sensors and Actuators B: Chemical. 2015;220:641-51.
48. Rad AS, Valipour P, Gholizade A, Mousavinezhad SE. Interaction of SO2 and SO3 on terthiophene (as a model of polythiophene gas sensor): DFT calculations. Chemical Physics Letters. 2015;639:29-35.
49. Shokuhi Rad A, Esfahanian M, Maleki S, Gharati G. Application of carbon nanostructures toward SO2and SO3adsorption: a comparison between pristine graphene and N-doped graphene by DFT calculations. Journal of Sulfur Chemistry. 2016;37(2):176-88.
50. Rad AS, Shabestari SS, Mohseni S, Aghouzi SA. Study on the adsorption properties of O 3 , SO 2 , and SO 3 on B-doped graphene using DFT calculations. Journal of Solid State Chemistry. 2016;237:204-10.
51. Shokuhi Rad A, Ghasemi Ateni S, Tayebi H-a, Valipour P, Pouralijan Foukolaei V. First-principles DFT study of SO2and SO3adsorption on 2PANI: a model for polyaniline response. Journal of Sulfur Chemistry. 2016:1-10.
52. Shokuhi Rad A, Zareyee D. Adsorption properties of SO 2 and O 3 molecules on Pt-decorated graphene: A theoretical study. Vacuum. 2016;130:113-8.
53. Rad AS, Mirabi A, Peyravi M, Mirzaei M. Nickel-decorated B12P12 nanoclusters as a strong adsorbent for SO2 adsorption: Quantum chemical calculations. Canadian Journal of Physics. 2017;95(10):958-62.
54. Rad AS, Ayub K. O 3 and SO 2 sensing concept on extended surface of B 12 N 12 nanocages modified by Nickel decoration: A comprehensive DFT study. Solid State Sciences. 2017;69:22-30.
55. Hohenberg P, Kohn W. Inhomogeneous Electron Gas. Physical Review. 1964;136(3B):B864-B71.
56. Kohn W, Sham LJ. Self-Consistent Equations Including Exchange and Correlation Effects. Physical Review. 1965;140(4A):A1133-A8.
57. The code, OPENMX, pseudoatomic basis functions, and pseudopotentials are available on a web site 'http://www.openmxsquare.org'.
58. Perdew JP, Burke K, Ernzerhof M. Generalized Gradient Approximation Made Simple [Phys. Rev. Lett. 77, 3865 (1996)]. Physical Review Letters. 1997;78(7):1396-.
59. Kokalj A. Computer graphics and graphical user interfaces as tools in simulations of matter at the atomic scale. Computational Materials Science. 2003;28(2):155-68.
60. Momma K, Izumi F. VESTA 3for three-dimensional visualization of crystal, volumetric and morphology data. Journal of Applied Crystallography. 2011;44(6):1272-6.